Electronic Supplementary Information (ESI)

Regular assembly of cage siloxanes by hydrogen bonding of dimethylsilanol groups

Naoto Sato, Yoshiyuki Kuroda, Takuya Abe, Hiroaki Wada, Atsushi Shimojima,*

Kazuyuki Kuroda*

Materials

The following chemicals were used without further purification: tetraethoxysilane (TEOS, Wako Pure Chemical Co. Ltd., ≥95.0%), tetramethylammonium hydroxide pentahydrate (TMAOH $5H_2O$, Aldrich, ≥95.0%), ethanol (Junsei Chemical Co. Ltd., 99.5%), chlorodimethylsilane (Tokyo Chemical Industry Co., Ltd., >95.0%), hexane (Kanto Chemical Co. Ltd., >96.0%), methanol (Wako Pure Chemical Co. Ltd., ≥99.8%), acetonitrile (Wako Pure Chemical Co. Ltd., ≥99.5%), palladium 5% on carbon (Tokyo Chemical Industry Co., Ltd., wetted with ca. 55% water), tetrahydrofuran (THF, Wako Pure Chemical Co. Ltd., ≥99.5%), magnesium sulfate (Wako Pure Chemical Co. Ltd., ≥98.0%), 2-methyltetrahydrofuran (Tokyo Chemical Industry Co., Ltd., ≥98.0%, stabilized with BHT), diethyl ether (Wako Pure Chemical Co. Ltd., ≥99.5%), toluene (Wako Pure Chemical Co. Ltd., ≥99.5%), and 1,3,5-trimethylbenzene (Tokyo Chemical Industry Co., Ltd., >97.0 %).

Synthesis of cubic siloxane modified with $SiMe_2H$ groups

Cubic octameric silicate ions ($Si_8O_{20}^{8-}$) were synthesized from a mixture of TEOS, TMAOH, ethanol and water, following our previous report (Y. Hagiwara, A. Shimojima and K. Kuroda, *Chem. Mater*., 2008, **20**, 1147). The selective formation was confirmed by ^{29}Si NMR (500 MHz, methanol-d_4, δ = –99.02). Evaporation of water gave hydrated crystals of $TMA_8(Si_8O_{20})$. The crystals (23.4 g) were dissolved in 30 mL of methanol, and the mixture was added to a hexane solution of chlorodimethylsilane (50 mL in 50 mL of hexane). The molar ratio of $HSiMe_2Cl$ to $Si_8O_{20}^{8-}$ was 32. After stirring the biphasic mixture at room temperature for 1 h, the upper phase was separated and solvents were evaporated in *vacuo*. The white solids were washed with acetonitrile to give dimethylsilylated cubic siloxane. ^{1}H NMR (500 MHz, $CDCl_3$): δ = 0.28 (*d*, 6H, SiC*H*$_3$), 4.74(m, 1H, Si*H*); ^{13}C NMR (126 MHz, $CDCl_3$): δ = 0.07; ^{29}Si NMR (99 MHz, $CDCl_3$): δ = –1.41, –108.64.

Synthesis of cubic siloxane modified with $SiMe_2OH$ groups (1)

Dimethylsilylated cubic siloxane (1.016 g, 1 mmol) and Pd/C (0.025 g) were mixed in tetrahydrofuran, followed by addition of H_2O (0.18 mL, 10mmol). After stirring at 40 °C overnight, the mixture was dried with magnesium sulfate and filtered with Celite® using diethyl ether as eluent. The resulting clear solution was concentrated by evaporation, and then added dropwise into hexane to form white precipitates. The precipitates were recovered by filtration, and recrystallized by slow evaporation from the solution of 2-methyltetrahydrofuran and toluene. ^{1}H NMR (500 MHz, tetrahydrofuran-d_8): δ = 0.10 (s, SiC*H*$_3$), 5.45 (br, SiO*H*), ^{13}C NMR (126 MHz,

tetrahydrofuran-d_8): δ = 0.07, ^{29}Si NMR (99 MHz, tetrahydrofuran-d_8): δ = –11.35, –109.45, MALDI TOF-MS: $[M + Na]^+$ = 1167.4 (calcd. 1166.9).

Characterization

Liquid-state ^{1}H, ^{13}C and ^{29}Si nuclear magnetic resonance (NMR) spectra were recorded on a Bruker AVANCE 500 spectrometer with resonance frequencies of 500.0 MHz, 125.7 MHz and 99.3 MHz, respectively, at ambient temperature using 5 mm glass tubes. Tetramethylsilane was used as an internal reference at 0 ppm. $CDCl_3$, methanol-d_6 and tetrahydrofuran-d_8 were used to obtain lock signals. A small amount of $Cr(acac)_3$ (acac = acetylacetonate) was also used as a relaxation agent for ^{29}Si nuclei. ^{13}C and ^{29}Si NMR spectra were measured with recycle delays of 2 s and 10 s respectively. Solid-state ^{29}Si magic angle spinning (MAS) NMR spectra were recorded on a JEOL JNM-ECX 400 spectrometer with resonance frequency of 99.5 MHz with 45° pulse and relaxation delay of 100 s. The samples were put in a 4 mm zirconia rotor. Matrix-assisted laser desorption/ionization (MALDI TOF-MS) spectra were recorded on a Bruker Autoflex instrument with dithranol as a matrix and sodium trifluoroacetate as a cationization agent. Transmission electron microscopy (TEM) images were taken on a JEOL JEM-2010 microscope operating at 200 kV. Scanning electron microscopy (SEM) images were taken on HITACHI S5500 operated at an acceleration voltage of 3 kV. The samples for TEM measurements were suspended in hexane, and the suspensions were dropped and dried on a carbon-coated micro-grid (Okenshoji Co.) which looks a cellular structure as observed in Fig.2(a), Fig. 3(b), and Fig. 4(c). The samples for SEM measurements were prepared with the same way as those for TEM measurements, or directly putting on a carbon tape. Optical

microscope images were taken on OLYMPUS EX51 apparatus. Powder X-ray diffraction (XRD) measurements were performed on a RINT-Ultima III diffractometer with Cu Kα radiation. IR spectra were obtained with a JASCO FT/IR-6100 spectrometer by KBr method. Thermogravimetry-differential thermal analysis (TG-DTA) curves were measured on a RIGAKU Thermo plus EV02 instrument under a dry-air flow with a heating rate of 10 °C/min.

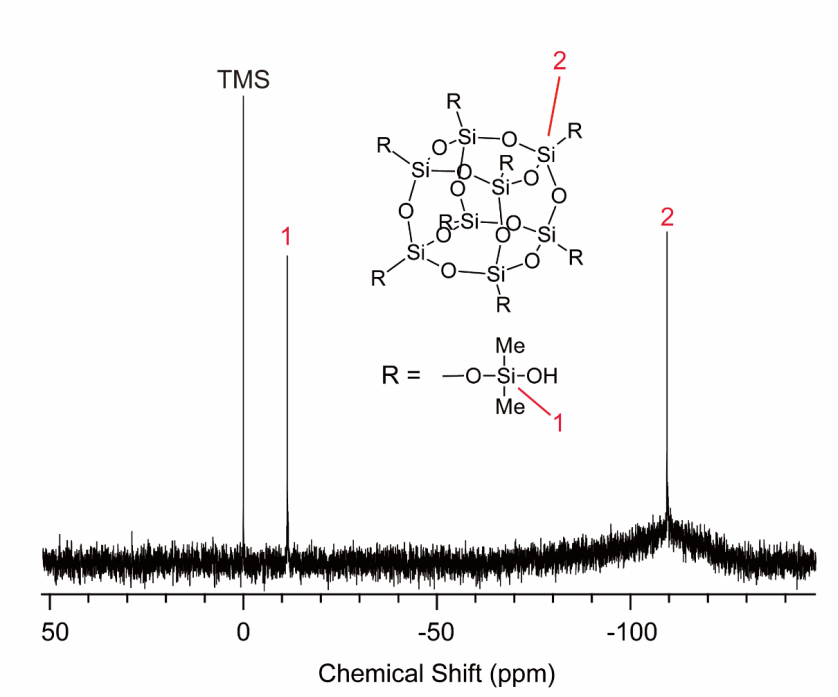

Fig. S1 Liquid-state ^{29}Si NMR spectrum of **1** dissolved in THF-d_8.

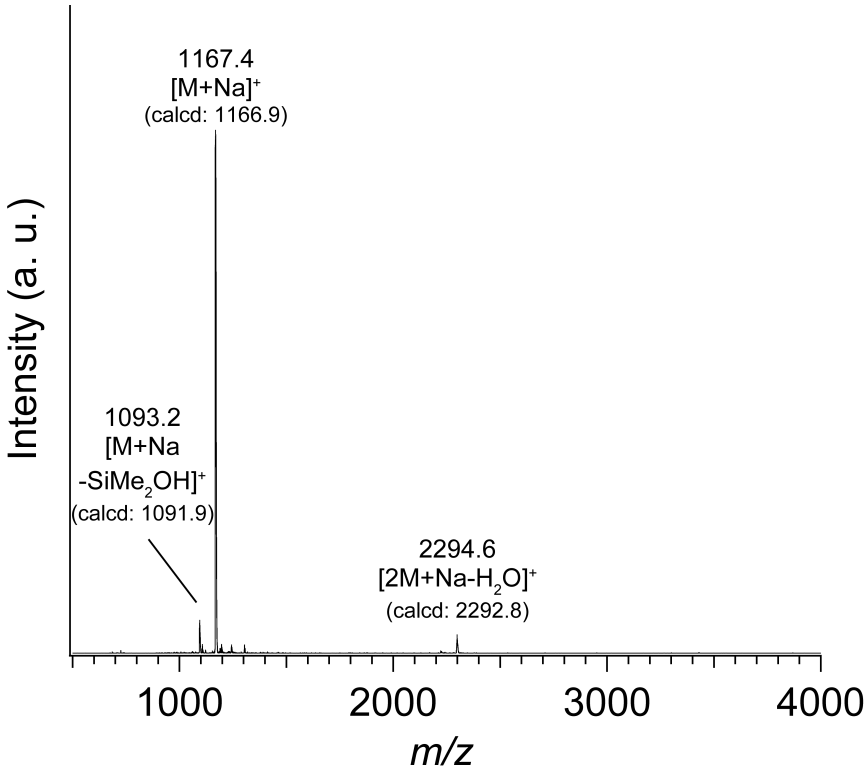

Fig. S2 MALDI-TOF MS spectrum of **1**. In addition to **1**, a small peak of a dimer formed by dehydration condensation of **1** (*m*/z = 2294.6) is detected. This is probably formed during ionization because the dimer was not detected by ^{29}Si NMR (Fig. S1).

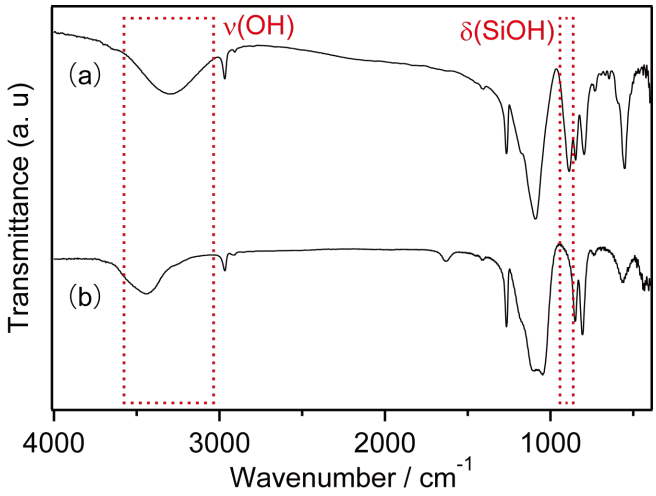

Fig. S3 FT-IR spectra of the crystals of **1** (a) before and (b) after heat treatment.

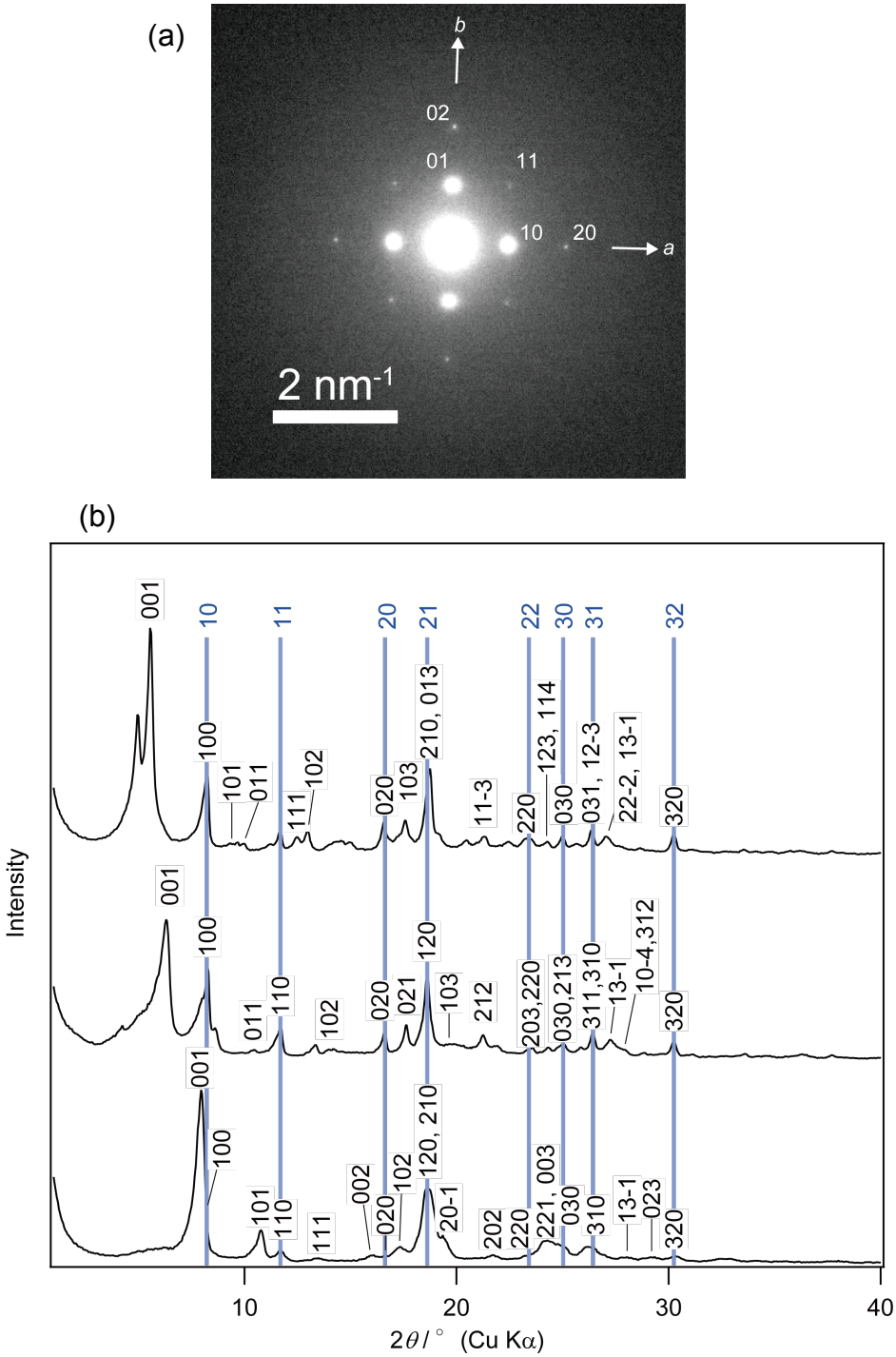

Fig. S4 (a) ED pattern of **1** after drying for 10 h. The incident electron beam is normal to the basal plane. (b) XRD patterns of the crystals of 1 before drying (top), after drying for 1 h (middle) and 10 h (bottom). Blue lines and their indices show the angles and assignments of the peaks corresponding to the two dimensional lattice observed in ED pattern(a), respectively.

Discussion on Fig. S4 (analysis of the diffraction data)

The ED pattern taken along the axis normal to the basal plane (Fig. S4(a)) indicates square arrays of distinct spots with tetragonal symmetry, indicating that molecules **1** are arranged in square lattice in the in-plane direction. The lattice constants were estimated to be $a = b = ca$. 1.07 nm. According to the two-dimensional structure, several peaks in the XRD patterns were assigned to the 10, 11, 20, 21, 22, 30, 31, and 32 diffractions which are shown by the vertical blue lines in the Figure S4(b). The 10 peak in the XRD pattern of **1** after drying for 10 h is difficult to be resolved because of the overlapping with the peak at d=1.11 nm; however, the observation of the higher order peaks strongly suggests that the 10 peak is present at d=1.07 nm. Such peaks due to the two-dimensional structure were observed, being independent of the drying period. Therefore, it is suggested that the two-dimensional arrangement of **1** within the a–b plane was not affected by the drying. The other peaks are possibly due to the diffractions associated with the structures along the c direction. In the case of **1** after drying for 10 h, most of the peaks were roughly attributable to a monoclinic lattice with the lattice constants $a = b$ = 1.07 nm, c = 1.12 nm, and β = 96.9°. The peaks ($l \neq 0$) were not found in the XRD patterns of **1** after drying for 1 h and before drying. The observed peaks in the XRD patterns were also roughly attributable to the monoclinic lattices (for **1** after drying for 1 h, $a = b$ = 1.07 nm, c = 1.40 nm, and β = 98.0°, and for **1** before drying, $a = b$ = 1.07 nm, c = 1.60 nm, and β = 97.2°). Several peaks are not assignable to the structures, which is probably due to intermediate phases. These analyses suggest that only out-of-plane structure (c and β values) changed during the drying. Such a behavior is quite similar to that of layered compounds accommodating solvent molecules in the interlayer galleries, whose interlayer distances decrease along with the progress of the evaporation of the solvent molecules from the interlayer.

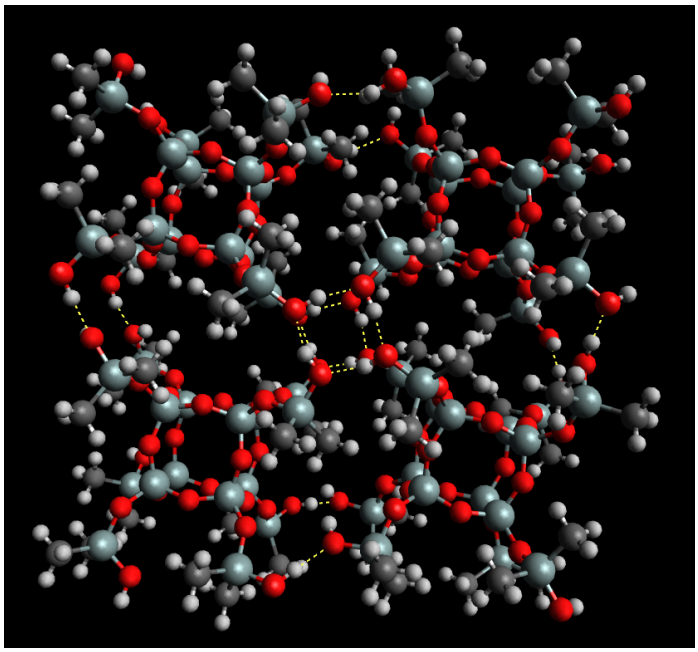

Fig. S5 Structural model of hydrogen bonds in the crystal of **1**. Light gray, dark gray, red and white spheres show silicon, carbon, oxygen, and hydrogen atoms, respectively. Dotted lines show hydrogen bonds. The model was made with Avogadro 1.11. 3. (M. D. Hanwell, D. E. Curtis, D. C. Lonie, T. Vandermeersch, E. Z. and G. R Hutchison, *J. Cheminf.*, 2012, **4**, 17)

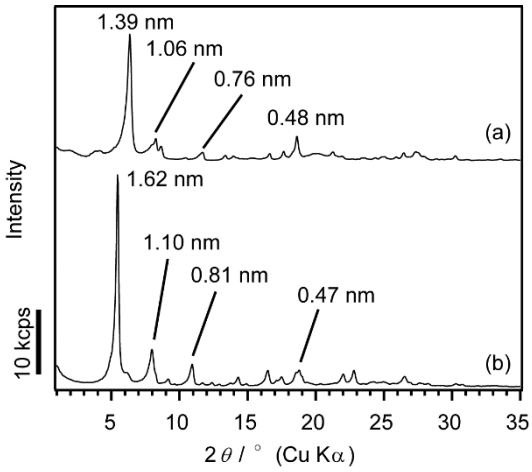

Fig. S6 Powder XRD patterns of (a) the crystals of **1** showing the main peak at 1.39 nm and (b) the same sample after treated with trimethylbenzene.

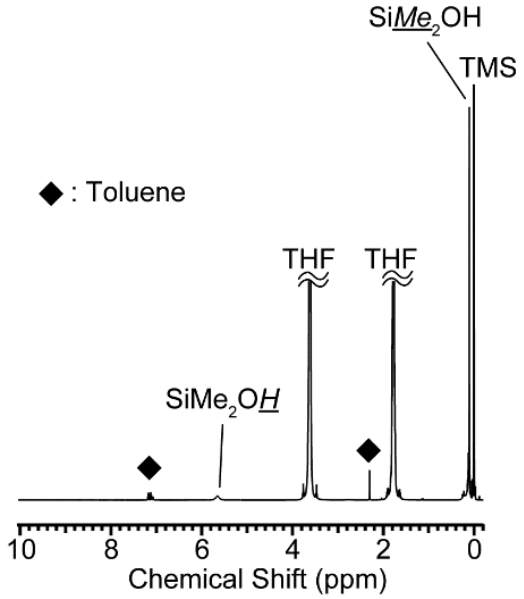

Fig. S7 Liquid-state ^{1}H NMR spectrum of the sample shown in **Fig. S4**(a) dissolved in THF-d_8.

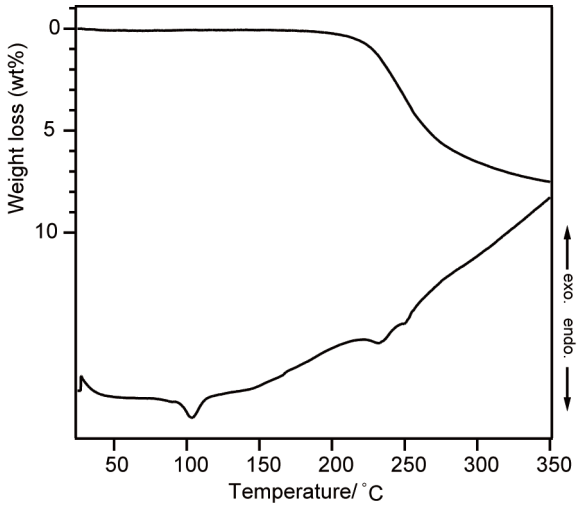

Fig. S8 TG-DTA curves of the sample shown in **Fig.S4**(a).

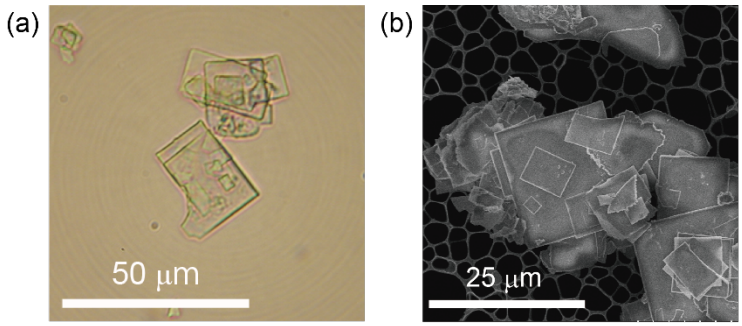

Fig. S9 (a) Optical microscopy image and (b) FE-SEM image of the crystals of **1** after heatin8 at 150 °C for 8 d.

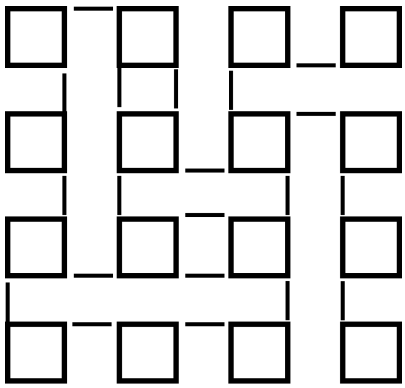

Fig. S10 A possible configuration of the interconnected network formed by polycondensation of silanol groups of **1**.

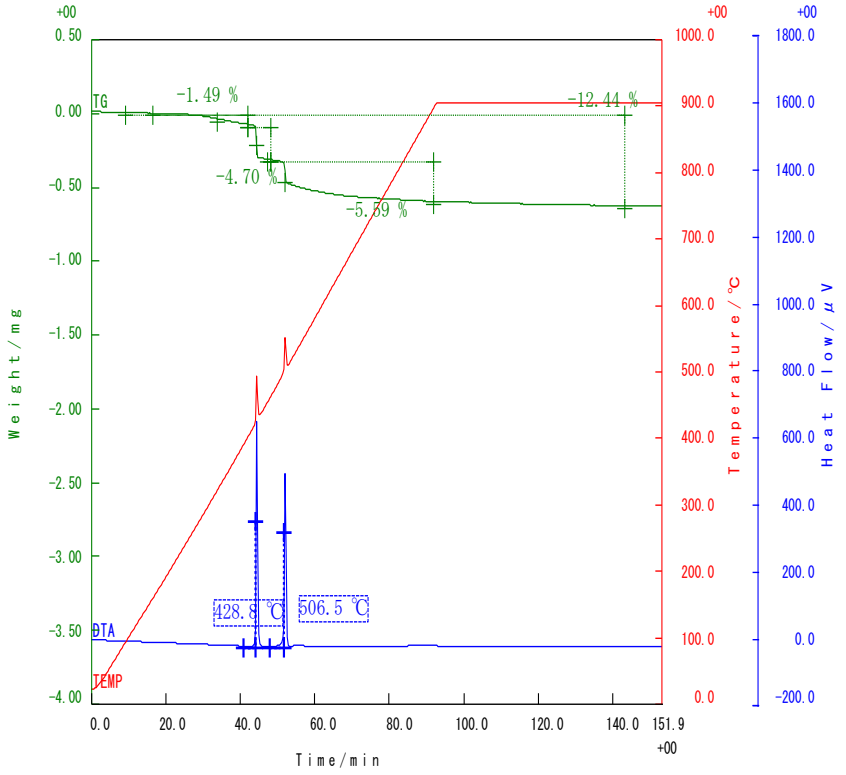

Fig. S11 TG-DTA curves of **1** after heating at 150 °C for 8 d.

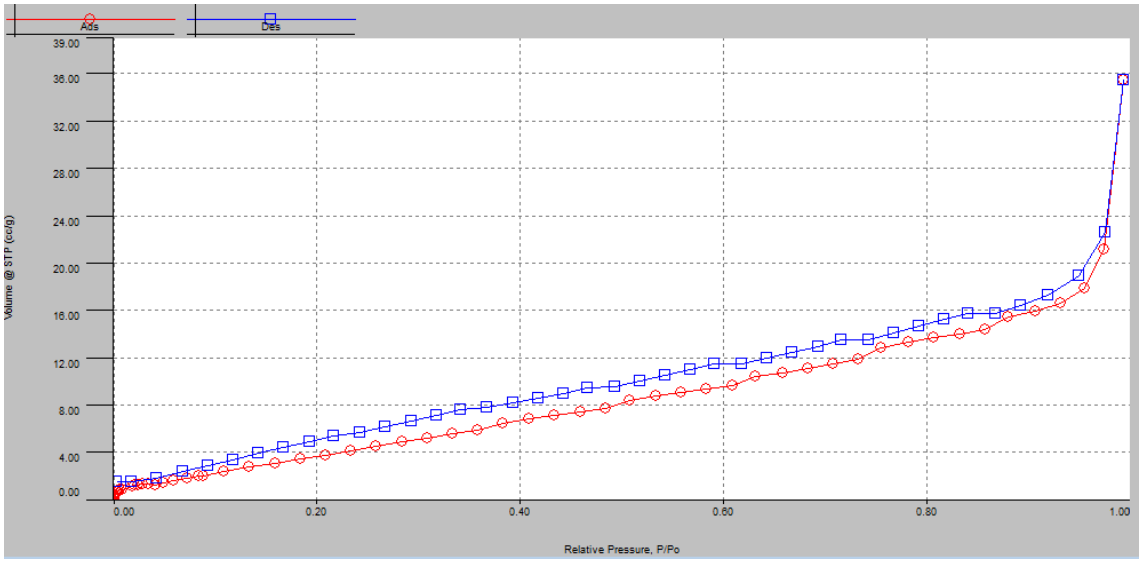

Fig. S12 N_2 adsorption-desorption isotherm of **1** after heating at 150 °C for 8 d.